



The influence of the synoptic regime on stable water isotopes in precipitation at Dome C, East Antarctica

5 Elisabeth Schlosser^{1,2}, Anna Dittmann¹, Barbara Stenni³, Jordan G. Powers⁴, Kevin W. Manning⁴, Valérie Masson-Delmotte⁵, Mauro Valt⁶, Anselmo Cagnati⁶, Paolo Grigioni⁷ and Claudio Sarchilli⁷

¹Inst. of Atmospheric and Cryospheric Sciences, University of Innsbruck,
10 Innsbruck, Austria

²Austrian Polar Research Institute, Vienna, Austria

³Department of Environmental Sciences, Informatics and Statistics, Ca 'Foscari University of
Venice, Venice, Italy

⁴National Center for Atmospheric Research, Boulder, CO, USA

15 ⁵Laboratoire des Sciences du Climat et de l'Environnement, Gif-sur-Yvette, France

⁶ARPA Center of Avalanches, Arabba, Italy

⁷Laboratory for Observations and Analyses of the Earth and Climate, ENEA, Rome, Italy

20

25

Correspondence to: Elisabeth Schlosser (Elisabeth.Schlosser@uibk.ac.at)

30



Abstract. The correct derivation of paleotemperatures from ice cores requires exact knowledge of all processes involved before and after the deposition of snow and consecutive
5 formation of ice. At the Antarctic deep ice core drilling site Dome C, a unique data set of daily precipitation amount, type and stable water isotope ratios is available that enables us to study atmospheric processes that influence the stable water isotope ratio of precipitation in detail. Meteorological data from both automatic weather station and a mesoscale atmospheric model were used to investigate how different atmospheric flow patterns determine the
10 precipitation parameters. A classification of synoptic situations that cause precipitation at Dome C was established and, together with back-trajectory calculations, was utilized to estimate moisture source areas. With the resulting source area conditions (wind speed, sea surface temperature (SST) and relative humidity) as input, the precipitation stable isotopic composition was modelled using the so-called Mixed Cloud Isotope Model (MCIM). The
15 model generally underestimates the depletion of ^{18}O in precipitation. It was shown that, contrary to the assumption widely used in ice core studies, a more northern moisture source does not necessarily mean stronger isotopic fractionation. This is due to the fact that snowfall events at Dome C are often associated with warm air advection due to amplification of planetary waves, which considerably increases the site temperature and thus reduces the
20 temperature difference between source area and deposition site. Also, no correlation was found between relative humidity at the moisture source and the deuterium excess in precipitation. The significant difference in the isotopic signal of hoar frost and diamond dust was shown to disappear after removal of seasonality.

1 Introduction

25

Ice cores from the vast ice sheets of Greenland and Antarctica have proven to be of high value in paleoclimate research. Of particular importance is the use of stable water isotope ratios as proxy for deriving past temperatures. However, it has been shown that the calibration of the “paleothermometer” is not as straightforward as originally assumed. Various factors apart
30 from air temperature influence the stable isotope ratio, both before and after the deposition of the snow that develops into ice by metamorphosis. Post-depositional processes were thought to occur mainly within the snow pack, firn or ice. Recent studies have shown, however, that the interaction between the uppermost layers of the snowpack and the overlying atmosphere



between precipitation events also plays an important role (Steen-Larsen et al., 2013; Bonne et al., 2013). In this study we focus on the processes before deposition, namely atmospheric processes related to moisture transport and precipitation formation. Since the stable water isotope ratio changes during evaporation and condensation processes (Dansgaard, 1964), it is important to know as much as possible about the history of the precipitation observed at an ice core drilling site, specifically moisture source, moisture transport paths, and meteorological conditions at both the moisture source and the deposition site. Precipitation measurements in Antarctica are rare due to the large technical difficulties of measuring precipitation at extremely low temperatures or high wind speeds. However, at the deep-drilling location Dome C on the East Antarctic plateau, a series of precipitation data has been collected that includes not only precipitation amounts but also precipitation type and stable isotope ratios. This unique data set can be combined with a full meteorological data set including radiosonde data, AWS data, and atmospheric model data. This, for the first time, allows us to study in detail the synoptic conditions that lead to precipitation at Dome C and how they are related to the precipitation stable isotope ratios.

2 Study site

Dome C (75.106 °S, 123.346 °E) is one of the major domes in East Antarctica, at an elevation of 3233 m. Since 2005, a wintering base has been operated there jointly by France and Italy (“Dome Concordia”). Dome C has a mean annual temperature of -54.5 °C and a mean annual accumulation of 25 mm water equivalent (w.e.), the latter derived from ice cores. Dome C is the site where the so far oldest ice has been retrieved during the European Project for Ice Coring in Antarctica (EPICA). After the first core, with a depth of 906 m covering ca. 32 000 years, had been drilled in 1977/78 (Lorius et al., 1979), several cores followed, and in January 2006, the EPICA drilling was completed at a depth of 2774.15 m, yielding ice approximately 800 000 years old. This core thus covers eight glacial cycles (EPICA community members, 2004), which doubles the time span that had been represented in ice cores previously.



3 Previous work

3.1 Stable isotopes

5 Since the ground-breaking work of Dansgaard (1964) stable water isotopes have become one
of the most important parameters measured in ice cores. An empirical linear relationship was
found between the annual mean air temperature (derived from the 10m-snow temperature)
and the annual mean $\delta^{18}\text{O}$ of snow samples along traverses in Antarctica and Greenland
(Jouzel et al., 1997). However, it became clear fairly early that this spatially derived
10 relationship was different from the corresponding temporal relationship and thus could not be
used as calibration for calculating paleotemperatures from ice core stable isotope ratios (e.g.
Masson-Delmotte et al., 2008). More recently it has been found, that the temporal relationship
is not constant for different climates or even time periods within a glacial or interglacial (Sime
et al., 2009). Spatial differences in the temporal relationship are common, and the relationship
15 can vary with season (e.g. Kuettel et al., 2012). While the empirical equation relates the stable
isotope ratio only to the condensation temperature at the deposition site, various other factors
influence this ratio, such as moisture source conditions and vertical and horizontal transport
paths, entrainment of additional moisture along the way, sea ice conditions, seasonality and
intermittency of precipitation as well as postdepositional processes. The second-order
20 parameter deuterium excess ($d = \delta\text{D} - 8 \cdot \delta^{18}\text{O}$), which combines the information from $\delta^{18}\text{O}$ and
deuterium, has been used to derive information about both condensation temperature and
moisture source conditions, namely wind speed, SST, and relative humidity (e.g. Stenni et al.,
2001). Most recently, due to the development of new measuring techniques, the rare isotope
 ^{17}O and the corresponding ^{17}O -excess have been introduced into ice core studies (e.g. Landais
25 et al., 2008, 2012; Schoenemann et al., 2014). The ^{17}O -excess is supposed to be insensitive to
evaporation temperature and less sensitive than d-excess to equilibrium fractionation
processes during formation of precipitation. Thus it may offer the potential of disentangling
the different effects of fractionation during evaporation, moisture transport, and precipitation
formation (Schoenemann et al., 2014).

30 A variety of models is used to simulate isotopic fractionation, from simple Rayleigh-type
distillation models to fully three-dimensional atmospheric circulation models. So far, most
models are still based on the early theories developed by Jouzel and Merlivat (1984). Ciais et



al. (1994) extended this theory to mixed clouds in their Mixed Cloud Isotope Model (MCIM), which is described further in the methods section.

Kavanaugh and Cuffey (2003) developed a model of intermediate complexity (ICM), more complex than simple Rayleigh-type models, but not as sophisticated as General Circulation
5 Models (GCM) to study how variations in single climate parameters or in fundamental characteristics of isotopic distillation affect the stable isotope ratio of polar precipitation. Schoenemann and Steig (2016) applied their model to ^{17}O -excess, using data from Vostok and the WAIS core for comparison. GCMs are so far not able to correctly represent d-excess or
10 ^{17}O -excess measured at Dome C (Stenni et al., 2010). In a most recent study, Steen-Larsen et al. (2017) evaluated various isotope enabled GCMs against in situ atmospheric water vapour isotope measurements. They found that, apart from a poor performance of all models for d-excess, biases in $\delta^{18}\text{O}$ could not be explained simply by model biases in air temperature and humidity.

In the discussion of sea level rise, often the possibility of a mitigation of sea level rise by
15 increased Antarctic precipitation, the most important component of the surface mass balance (SMB) is mentioned (e.g. Church et al, 2013). However, the relationship between stable isotope ratios and precipitation/accumulation is not fully understood yet. Commonly, the assumption of a positive correlation between stable isotope ratio (as proxy for air temperature) and accumulation rate was used based on the relationship between temperature and saturation
20 water vapour pressure (Clausius-Clapeyron). However, contrasting results are found in the recent literature. While Frieler et al. (2015), using both model and ice core data, state that Antarctic accumulation increases with rising air temperature, Fudge et al. (2016) found that the relationship between accumulation and temperature has not been constant over the past 30000 years in West Antarctica. They stated that atmospheric dynamics play a more
25 important role than thermodynamics, which had also been found by Altnau et al. (2015) and Schlosser et al. (2014) in coastal Dronning Maud Land.

3.2 Synoptic analysis

30 In the past, precipitation in the interior of the Antarctic continent was only poorly understood because only a few meteorological observatories exist in continental Antarctica and analysis of satellite imagery has brought only limited progress due to the difficulty of distinguishing between clouds and the snow surface (Massom et al., 2004). Since the improvement of global



and mesoscale atmospheric models, however, our knowledge has advanced considerably. Noone et al. (1999) studied precipitation conditions in Dronning Maud Land (DML) using ECMWF reanalysis data. They found that 89 % of the days have low (<0.2 mm) precipitation, corresponding to 31 % of the annual total, whereas only 1 % of the days have high precipitation of more than 1mm per day, but account for 20 % of the annual precipitation. High precipitation days were shown to be connected to amplified upper level planetary waves that direct moist air towards DML. These results have been confirmed and extended by various authors for different parts of Antarctica. It has been shown that a few snowfall events per year can be responsible for up to half of the annual total precipitation (Braaten, 2000, Reijmer and Van den Broeke, 2003; Fujita and Abe, 2006; Schlosser et al., 2010a, Gorodetskaya et al., 2013). The synoptic events with blocking anticyclones were also described by Scarchilli et al. (2010), Massom et al. (2004), and Hirasawa et al. (2000). At the deep-drilling site Dome Fuji, the warm air advection combined with orographic lifting sometimes was not sufficient for precipitation formation, but did cause the removal of the prevalent temperature inversion layer by cloud formation that increased the downward long-wave radiation and by turbulent mixing (Enomoto et al. 1998; Hirasawa et al., 2000). Also, increased amounts of diamond dust can be observed after a synoptic snowfall event when moisture levels are still higher than on average (Hirasawa et al., 2013; Dittmann et al., 2016; Schlosser et al., 2016). Dittmann et al. (2016) investigated the only other daily precipitation/stable isotope ratio data set available in the interior of Antarctica, which was created in 2003 at the Japanese deep drilling site Dome Fuji (Fujita and Abe, 2006). They investigated synoptic conditions during precipitation, estimated moisture source areas for precipitation events and used MCIM to model the stable isotope ratios. Five typical weather situations for precipitation were defined. Approximately two thirds of the days were directly or indirectly related to advection of moist air associated with amplification of the planetary waves. The model represented the observed annual cycle of $\delta^{18}\text{O}$ and deuterium excess fairly well, but underestimated the amount of fractionation between first evaporation at the oceanic moisture source and deposition at Dome Fuji. Nicolas and Bromwich investigated intrusions of warm maritime air into West Antarctica (Nicolas and Bromwich, 2011). For ice core interpretation, these findings are important since they contradict the older assumption that precipitation in the interior Antarctica is predominantly diamond dust and thus exhibits only a weak seasonality. This would mean that all seasons are represented evenly in the ice core. If, however, the synoptic snowfall occurs preferably in certain seasons



and/or this preference is not constant in different climates, potentially a cold or warm bias would be found in the temperature derived from stable water isotopes of an ice core. Therefore an understanding of the atmospheric circulation and its influence on precipitation conditions at deep drilling sites is essential for a correct interpretation of the ice core proxy
5 data.

4 Data and methods

4.1 Precipitation and stable isotope data

10

Precipitation has been measured and sampled at Dome C since 2006 (with some interruptions in the early time period) and is ongoing. A wooden platform of approximately 1m height covered by a polystyrene/teflon plate is used to measure daily precipitation amounts. The elevated platform, which is surrounded by a rail of 5 cm height helps to avoid contributions
15 from low drifting snow, but cannot prevent that precipitated snow is removed completely - and thus not measured - at higher wind speeds. The platform is located at a distance of 800 m from the main station. Until the end of 2007, the measurements were not carried out daily, but the samples were collected only when precipitation reached a certain threshold, which led to sampling intervals of four to five days. Since December 2007, precipitation is sampled once
20 per day at 0100 UTC and amounts and stable isotope ratios of the samples are determined. In this study we therefore consider the time period 2008 – 2010, with the more recent samples having not yet been analysed at the time of our study.

The samples were stored frozen in sealed plastic bags until they were delivered to the Geochemistry Laboratory at University of Trieste, where they were melted and put into high-
25 density-polyethylene (HDPE) vials. Then they were stored at a temperature of approximately -20 °C until analysis. The stable isotope ratio was determined using mass spectrometry (Thermo-Fisher Delta Plus Advantage). When the precipitation amount did not reach 5ml, a PICARRO cavity ringdown spectroscope (CRDS) was employed (model L1102-i). The accuracy of the mass spectrometer is ± 0.05 ‰ for $\delta^{18}\text{O}$ and ± 0.7 ‰ for δD , the CRDS gives a
30 precision of ± 0.1 ‰ for $\delta^{18}\text{O}$ and ± 0.5 ‰ for δD . This yields a final precision for deuterium excess of ± 0.8 ‰ and ± 0.9 ‰ for mass spectrometry and CRDS, respectively. Measurable precipitation was observed on 59 % of all days, stable isotope ratios were determined on 45 % of the days.



Furthermore, the crystal type of the precipitation is analysed, so that diamond dust, drift snow and snowfall can be distinguished. Diamond dust forms due to radiative cooling of almost saturated air and consists of very fine needles. Mixing of a warmer, moister air mass with cold air can also lead to supersaturation of the cold air and consequent ice crystal formation.

5 Synoptic snowfall is marked by various types of snow crystals that depend mainly on air temperature during crystal formation, whereas drift snow can be recognised by broken crystals. Also, a mixing of crystal types can be observed. Note that the precipitation amounts are so small that errors in quantification can amount to 100 % or more. However, usually cases of diamond dust exhibit amounts one order of magnitude smaller than synoptic snowfall

10 events. So far, the Dome C precipitation series, complemented by stable isotope measurements represents the first and only multi-year precipitation series at an Antarctic deep-drilling site.

$\delta^{17}\text{O}$ and ^{17}O -excess have been determined for a part of the samples, but the amount of data is not sufficient yet to get statistically significant results, thus they are not used in the present

15 study.

A detailed description of the measurements and a first analysis of the stable isotope data can be found in Stenni et al. (2016).

20 **4.2 AWS and radiosonde data**

Radiosonde data from the meteorological station at Dome C are used to determine the temperature at the top of the surface inversion layer and the condensation level. The upper-air data are provided by the Meteo-climatological Observatory of the Italian Antarctic Research

25 Program (PNRA). Since the beginning of the measurements in 2005, a radiosonde is launched every day at 12 UTC, unless wind speeds are so high that a balloon start is impossible. For each standard pressure level, geopotential height, air temperature, humidity and wind are measured and the data are delivered as TEMP files to the WMO (World Meteorological Organisation) Global Telecommunication System (GTS).

30 The current Automatic Weather Station (AWS), named Dome C II, has been installed by the Antarctic Meteorological Research Center (AMRC) in 1995. The AMRC and AWS Program are sister projects of the University of Wisconsin-Madison, which are funded by the United States Antarctic Program (USAP). USAP provides real-time and archived weather observations and satellite measurements and supports a network of AWS across Antarctica.



At the AWS, standard meteorological variables, namely air temperature, surface pressure, wind speed and direction, and humidity are measured. The data can be found at <http://amrc.ssec.wisc.edu>.

5

4.3 AMPS archive data

The Antarctic Mesoscale Prediction System (AMPS) (Powers et al. 2012) is a real-time
10 numerical weather prediction system run to provide guidance for the weather forecasters of
the United States Antarctic Program (USAP). It has been operated by the National Center for
Atmospheric Research (NCAR) in support of the USAP since 2001, at first employing the
polar version of the Fifth-Generation Pennsylvania State University/NCAR Mesoscale Model
(Polar MM5). Since 2006 AMPS has used the Weather Research and Forecasting (WRF)
15 Model. The model performance of WRF in AMPS and in Antarctica has been verified in
previous studies (Bromwich et al. 2005; Bromwich et al. 2013; Deb et al. 2016), while model
output has supported various Antarctic investigations (e.g., Powers, 2007; Nigro et al., 2011;
2012). The AMPS Archive is the repository of gridded output from AMPS from over the
years (Powers et al., 2012), and WRF gridded output from the archive has supported a number
20 of studies (Seefeldt and Cassano, 2008; Schlosser et al., 2010a; Seefeldt and Cassano, 2012;
Schlosser et al., 2016). AMPS Archive data from the period 2008–2010 are used here in
analyses of the meteorological conditions affecting Dome C and its precipitation.

For the period analysed in this study, the AMPS WRF configuration consisted of a nested
domain setup with grids of 45-km and 15-km horizontal spacing covering from the Southern
25 Ocean poleward and the Antarctic continent, respectively. As the 15-km domain includes
Dome C, it is the output from this grid that is used for the analyses here. Vertical resolution in
WRF for the study period reflected 44 levels from the surface to 10 hPa. The use of the
AMPS archive data follows the methodology of a number of published studies analysing
conditions and regimes at ice core drilling sites across Antarctica (Schlosser et al., 2008;
30 Schlosser et al., 2010b; Schlosser et al., 2016; Dittmann et al., 2016).

In this study, AMPS archive data are utilized to investigate the synoptic situation that lead to
precipitation and to estimate moisture sources for the precipitation events. Fully three-
dimensional 5-day back trajectories were calculated with the RIP4 software (Stoelinga, 2009)



and together with 500 hPa geopotential fields used to estimate the moisture source. Conditions at the moisture source are then derived as input for the stable isotope modelling.

4.4 MCIM

5

The so-called Mixed Cloud Isotope Model (MCIM) is a simple Rayleigh-type model that, however, allows the co-existence of water droplets and ice crystals and, as such, is the consequent further development of the basic distillation model established by Jouzel and Merlivat (Jouzel and Merlivat, 1984; Merlivat and Jouzel, 1979). It is still widely used in ice
10 core studies and also is the basis for implementation of stable isotopes in General Circulation Models (GCM) or climate models. The model calculates fractionation in an isolated air parcel between the initial evaporation and the final precipitation. In contrast to a pure Rayleigh model, an adjustable part of the condensate stays in the cloud. In a likewise adjustable range of temperatures, both liquid droplets and ice crystals occur in the cloud, which causes
15 additional kinetic fractionation processes due to the Bergeron-Findeisen effect: because of the different saturation vapor pressure with respect to ice and water, the actual vapor pressure lies between the saturation vapor pressure above water and that above the ice. This means a sub-saturated environment for liquid water but a supersaturated environment for ice. This results in a net transport of water vapour from the droplets to the ice, with fractionation during
20 evaporation from the droplets and deposition (i.e. negative sublimation) on the ice crystals. The initial isotopic composition of the vapor after the first evaporation is calculated assuming a balance between evaporation and condensation. Details about MCIM can be found in Ciais et al. (1994) and Dittmann et al. (2016).

25 5 Results

5.1 Meteorological conditions at Dome C

Figure 1 shows a histogram of daily precipitation amounts at Dome C for the period 2008-
30 2010 derived from a) measurements and b) AMPS archive data. It shows an extreme L-distribution: in both model and observations, a large number of extremely small amounts are observed compared to only a few events with more than 0.2 mm. The 90 % and the 95 % percentiles are shown as possible thresholds for synoptically caused snowfall events. Note that the observational data refer basically to the precipitation sampling and cannot be



corrected for cases where the wind speed was so high that no sampling was possible because the snow had been blown away from, or not accumulated at all, at the platform. The small amounts most likely are associated with diamond dust formation, whereas the larger events are related to synoptically caused snowfall events (in the following called synoptic snowfall
5 events), which we will discuss in the next paragraph. Hoarfrost can have variable amounts depending on the amount of available moisture (see also Section 5.2). However, as can be seen in Fig. 2, hoarfrost mainly occurs in winter, at deep temperatures when absolute humidity is comparatively low.

Note that Fig. 2 only displays the number of days with the observed precipitation type, not
10 taking into account snowfall amounts. Snowfall days at higher temperatures are less frequent than those at temperatures below $-50\text{ }^{\circ}\text{C}$, but usually have considerably larger amounts of precipitation.

Figure 3 displays the wind direction at Dome C from the AWS for a) all days and b) only days
15 with wind speeds above 10 ms^{-1} . Dome C is the Antarctic station with the highest constancy in wind direction (Wendler and Kodama, 1984), even though no katabatic influence is found at the dome. Wind directions still show a preference for the SW sector, which can be explained by the climatological mean pressure distribution with an anticyclone prevailing above the continent that, on average, leads to approximately westerly to southerly winds at Dome C. For the higher wind speeds, the direction is much more variable, which
20 demonstrates that the prevailing anticyclonic weather conditions are disturbed more often than previously thought.

5.2 Synoptic patterns during precipitation

25 Based on mainly 500 hPa geopotential height from the AMPS archive, six different synoptic situations that lead to increased amounts of precipitation were classified. In Figure 4, examples for these six classes are displayed:

4a) Blocking anticyclone

30

Figure 4a shows the 500 hPa geopotential height field for 23 May 2007 00 UTC. A strong upper-level ridge is situated between $130\text{ }^{\circ}\text{E}$ and $160\text{ }^{\circ}\text{W}$, with the corresponding trough west of it and the ridge axis extending from NNW to SSE, which consequently brings Dome C into a strong northwesterly flow that originates at a latitude of approximately $45\text{ }^{\circ}\text{S}$. The relatively



warm and moist air from these latitudes is orographically lifted above the Antarctic continent, which leads to cooling and precipitation formation. Even though only a small fraction of the original moisture arrives at Dome C, it is enough to produce precipitation amounts about one order of magnitude larger than the more frequent diamond dust precipitation. The pattern
5 lasted from 22 to 26 May 2007 in almost the same configuration, thus led to a considerable amount of precipitation. The AMPS precipitation field (12h-36h forecast from 22 May 12 UTC corresponding to precipitation total for 23 May 00 UTC-24 UTC) is also shown. It can be clearly seen how precipitation decreases from the coast towards the interior, but still reaches the high plateau.

10

4b) Weak anticyclone with north-westerly flow

Figure 4b displays similar fields as in Fig. 4a, 500 hPa geopotential for 13 Feb 2007 00 UTC and the 24 h precipitation for 13 Feb. The high pressure ridge, situated slightly farther to the west than in the previous case, is of smaller meridional extent than in the Fig. 4a and is less
15 persistent, but principally the situation is fairly similar, with transport of moist, warm air in a northwesterly flow between an upper level ridge and a trough from areas south of 50 °S. Those situations occur fairly frequent (order of magnitude: once per month, with high inter-annual variability, though).

20 4c) Anticyclone with north-easterly flow

In Figure 4c a special case of the earlier examples is shown: the flow here is northeasterly rather than northwesterly. Often a cutoff low or upper level low is situated north or slightly northwest of the coast of Wilkes Land in this synoptic pattern. The flow is directed around the
25 cutoff low towards Dome C. While the distance to the coast is similar for a north-westerly and a northeasterly flow, some dynamic lifting of the air mass above the ocean might be involved in addition to the orographic lifting. This should be studied in a future investigation.

4d) Splitting of flow

30 In contrast to conditions determined from studies for Dome Fuji and Kohnen Station in Dronning Maud Land, Dome C relatively often experiences a situation where the planetary waves are amplified, but the flow is split into a zonal part, in which Dome C is situated, and a meandering part with the strong trough and ridge in the amplified flow staying north of the area. This leads to reduced advection of warm and moist air to Dome C, but can still cause



precipitation formation. The air mass originates farther south than in the cases described above, thus the meridional exchange of heat and moisture is smaller.

4e) Flow from West Antarctica

5 Another situation that has not been found at other deep drilling sites is that the relatively warm and moist air is advected to Dome C from the Amundsen-Bellingshausen Sea across Mary Byrd Land. In the 500 hPa geopotential height field in Figure 5e) a closed circulation centered in the Ross Sea can be seen, which leaves Dome C in a flow bringing air from the Amundsen Sea or north of it towards Dome C. For this situation, AMPS shows precipitation
10 only in the “vicinity” of Dome C, not at the station itself. This situation is most likely influenced by the strength and position of the Amundsen-Bellingshausen Seas Low (ASL, e.g. Raphael et al., 2016). Fig. 5 shows the AMPS sea level pressure for 3 May 2007. In the described case, the ASL is found in a rather western position, corresponding to its usual annual cycle, with the westernmost position in winter. A small, but strong core is found in the
15 western Amundsen Sea, accompanied by an upper level low. Together with a weaker, but broader low at surface and upper levels above the Ross Sea and beyond, this leads to a northerly flow at the eastern edge of the ASL, which is being continued over the continent towards Dome C.

20 4f) Post-event increased moisture

Several cases, for which AMPS shows very low or no precipitation, exhibit increased amounts of measured precipitation at Dome C. The precipitation was classified as diamond dust, but the events showed amounts that were non-typically high for this type of precipitation. It was
25 found that these cases, which did not show the northerly flow connected to advection of relatively warm and moist air, usually occurred after a synoptic snowfall event had happened. This means that the available moisture was still increased, and AMPS shows a fairly large, isolated area of weak precipitation almost centered at Dome C.

30 5.3 Wind speed and precipitation

The wind direction for synoptic precipitation events only, identified in the AMPS data, is displayed in Fig. 6. Contrary to the average conditions displayed in Fig. 3, with a pronounced preference of the southeast sector, for snowfall events the most frequent direction is NNW to



NW, with almost no cases from the SW sector. Also, the highest wind speeds ($12\text{-}14\text{ ms}^{-1}$) are observed from a northwesterly direction. AMPS data rather than AWS data are used for this figure because AMPS was utilized to identify the high-precipitation events. In the observations, many cases with high precipitation were not found because they were accompanied by high wind speeds, and thus no sampling of the precipitation was possible after the snow had been blown off the measuring platform. A study of the mismatches of AMPS and observation (i.e. where AMPS showed large precipitation amounts whereas no precipitation was found in the observations) revealed that those cases usually showed an increase in temperature and wind speed observed at the AWS, indicating a synoptic disturbance.

This also becomes clear from Figure 7, in which the relationship between precipitation amounts and wind speed is illustrated. Precipitation amounts are related to wind speed for a) observations and b) AMPS archive data. Again, it has to be considered that days with high wind are mostly related to synoptic snowfall events that have high precipitation amounts in AMPS, but cannot be seen in the observation since the snow has been blown off the measuring platform and thus not been measured. Thus, Fig. 7b) seems to be more realistic than Fig. 7a), with larger precipitation amounts at correspondingly higher wind speeds. Surface mass balance data from firm cores and a stake array suggest that AMPS precipitation has a positive bias, whereas the total amounts measured at the platform are too low, which seems plausible considering the above mentioned mass losses due to removal of snow from the platform by the wind. Since all three methods have considerable error possibilities, we refrain from a numeric quantification of these findings.

5.4 Isotope measurements and modelling

Figure 8a shows observed $\delta^{18}\text{O}$ vs. 2 m air temperature for the different types of precipitation: snow, diamond dust, and hoar frost. High-precipitation events, for which trajectories were calculated, are marked with circles. The regression lines differ only slightly for the various precipitation types. For all samples, a $\delta^{18}\text{O}$ -T slope of $0.49\text{ ‰/}^\circ\text{C}$ is found ($r=0.79$, $n=498$). The slope for the studied high-precipitation events only is $0.39\text{ ‰/}^\circ\text{C}$, lower than for all days ($r=0.78$, $n=21$). Also, the relationship between deuterium excess and $\delta^{18}\text{O}$ (Fig. 8b) shows no significant differences between the precipitation types.



In Figure 10 observed and modelled $\delta^{18}\text{O}$ and deuterium excess for days with moisture source estimates are displayed. Observed $\delta^{18}\text{O}$ and deuterium excess show a clear annual cycle. While $\delta^{18}\text{O}$ exhibits a clear maximum in summer, the deuterium excess peaks in winter, most clearly in 2010, which was least disturbed by warm air intrusions. For the modelling of isotopic fractionation with MCIM, initial conditions at the moisture sources derived from a 5 day back-trajectory calculation combined with the synoptic flow analysis were used following the method described in Dittmann et al. (2016). The moisture sources for arrival levels 600 hPa and 500 hPa are shown in Figure 9. Stronger colours correspond to higher frequency of occurrence of the respective moisture source. For cases, in which the trajectory left the AMPS domain, ECMWF interim-reanalysis data were used to estimate the moisture source. For both arrival levels, the moisture source is found mainly in the 90 °E - 130 °E longitude range of the Southern (Pacific) Ocean. The most frequent latitude ranges are 40 °S - 50 °S for 600 hPa arrival level, and 35 °S - 50 °S for the 500 hPa level. The model was run using different assumptions for the condensation temperature: i) moisture source conditions derived for the estimate using the 500 hPa back-trajectory: arrival temperature of the trajectory at the 500 hPa level (blue circles), ii) moisture source conditions derived for the estimate using the 600 hPa back-trajectory; arrival temperature at the 600 hPa level (red circles), and iii) moisture source estimated using the 500 hPa trajectory; arrival temperature at the upper limit of the inversion layer derived from radiosonde data (green circles). The modelled $\delta^{18}\text{O}$ values are generally too high, no matter which assumption is made for the condensation temperature. Using the 500 hPa data yields a smaller bias, but a lower correlation between the observed and modelled $\delta^{18}\text{O}$ than using the 600 hPa temperatures and moisture source assumptions. ($R=0.61$, bias=3‰ and $R=0.74$, bias=11.3 ‰ for 500 hPa and 600 hPa, respectively, $p<0.05$). The corresponding values for use of the inversion temperature are $R=0.66$ ($p<0.05$), bias = 10.5 ‰. An attempt to use the condensation temperature at Dome C derived from radiosonde data as model input (rather than inversion temperature or temperature at the arrival levels of the calculated trajectories) did not improve the correlation between observed and modelled isotope ratios: no statistically significant correlation between modelled and observed $\delta^{18}\text{O}$ was found in this case. Modelled and observed deuterium excess show a weak correlation only when the inversion temperature is used as condensation temperature ($R=0.51$, $p=0.02$).



6 Discussion and Conclusion

The first and only multi-year data series of daily precipitation amounts, precipitation type and stable isotope ratios was combined with data from a mesoscale atmospheric model and a
5 simple isotope model to study the influence of the precipitation regime on the corresponding stable water isotope ratios.

Snowfall events with precipitation amounts an order of magnitude larger than diamond dust precipitation were often associated with amplification of Rossby waves in the circumpolar trough with increased meridional transport of heat and moisture. In contrast to other deep
10 drilling sites in East Antarctica, at Dome C in some cases a moisture transport from West Antarctica across the continent occurred. Increased diamond dust precipitation was observed after such event-type snowfall when the remaining moisture was still increased. Note that diamond dust is not parameterized in the WRF model used in AMPS. Nevertheless the model yields only 6 days with no precipitation at all in the study period.

15 The $\delta^{18}\text{O}$ -T relationship did not differ between the different precipitation types: snowfall, diamond dust and hoar frost showed almost similar slopes. Hoar frost exhibited significantly lower $\delta^{18}\text{O}$ and δD values and higher deuterium excess than snowfall and diamond dust, however, this is most likely due to the fact that hoarfrost occurs mainly in winter at very low temperature. The local cycle of sublimation and deposition of hoar frost is still fairly
20 unknown, but seems to be a process where the depletion and enrichment of heavier isotopes are reversible. This basically leads to the conclusion that since there is no moisture source on the continent, the moisture responsible for diamond dust and hoar frost formation has to be transported on similar pathways as synoptic snowfall to the interior of the continent.

Modelled stable isotope ratios showed a “warm” bias compared to the observations. Using the
25 condensation temperature at Dome C derived from radiosonde data as model input (rather than the temperature at the top of the inversion layer or the temperature at the arrival levels of the calculated trajectories) did not improve the correlation between observed and modelled isotope ratios; in fact, the correlation coefficient decreased considerably and was no longer significant, most likely due to the fact that the condensation temperature determined from the
30 radiosonde data displayed only a weak annual cycle. More detailed studies of vertical humidity and temperature profiles during precipitation are necessary to understand this result. At present, no explanation for this can be offered. The general assumption that the temperature at the top of the inversion layer represents the condensation temperature could not be proven. No correlation was found between observed deuterium excess and relative



humidity at the estimated moisture source, which is contradictory to the commonly used assumptions in the literature.

It was also found that a more northern moisture source does not – as commonly assumed - necessarily mean stronger depletion of heavy isotopes, since the advection of warm air associated with snowfall events reduces the temperature difference between oceanic moisture source and deposition site and thus the strength of the distillation. This confirms the recent results of Dittmann et al. (2016) found at the deep drilling site Dome Fuji.

Author contribution:

10

Barbara Stenni is responsible for the precipitation measurements and stable isotope analysis, Mauro Valt and Anselmo Cagnati for the crystal analysis, and Paolo Grigioni and Claudio Sarchilli for the radiosonde data provision and analysis. Anna Dittmann carried out the stable isotope modelling, with contributions by Valerie Masson-Delmotte, as well as the comparisons of observations with modelled meteorological and isotope data. Elisabeth Schlosser did the analysis of synoptic patterns, where AMPS data analysis was supported by Jordan Powers and Kevin Manning. The manuscript was prepared by Elisabeth Schlosser, Anna Dittmann, Jordan Powers, and Kevin Manning with constructive comments of the other co-authors.

20

Acknowledgements

This study was funded by the Austrian Science Funds (FWF) under grants P24223 and P28695. AMPS is supported by the U.S. National Science Foundation, Division of Polar Programs. The precipitation measurements at Dome C have been carried out in the framework of the Concordia station and ESF PolarCLIMATE HOLOCLIP projects. We appreciate the support of the University of Wisconsin-Madison Automatic Weather Station Program with the Dome C II data set (NSF grant numbers ANT-0944018 and ANT-12456663). Radiosonde data and information were obtained from IPEV/PNRA Project “Routine Meteorological Observation at Station Concordia – www.climantartide.it. We would like to express our gratitude to all winterers at Dome C, who were involved in the precipitation sampling.



References

- Bonne, J. L. , Steen-Larsen, H. C. , Risi, C. , Werner, M. , Sodemann, H. , Lacour, J. L. , Fettweis, X. , Cesana, G. , Delmotte, M. , Cattani, O. , Vallelonga, P. , Kjaer, H. A. ,
5 Clerbaux, C. , Sveinbjörnsdóttir, Á. E. and V. Masson-Delmotte: The summer 2012 Greenland heat wave: In situ and remote sensing observations of water vapour isotopic composition during an atmospheric river event. *J. Geophys. Res.*, 120 (7), 2970-2989, 2015. doi:10.1002/2014JD022602.
- 10 Braaten, D. A.: Direct measurements of episodic snow accumulation on the Antarctic polar plateau. *J. Geophys. Res.*, 105, (D9) 10,119-10,128, 2000.
- Bromwich, D. H., Monaghan, A. J., Manning, K. W., and Powers, J. G.: Real-time forecasting for the Antarctic: An evaluation of the Antarctic Mesoscale Prediction System (AMPS), *Mon. Weather Rev.*, 133, 579-603, 2005.
- 15 Bromwich, D. H., Otieno, F. O., Hines, K. M., Manning, K. W., and Shilo, E.: Comprehensive evaluation of polar weather research and forecasting performance in the Antarctic. *J. Geophys. Res.*, 118, 274–292, doi:10.1029/2012JD018139, 2013.
- Church, J.A., et al.: Sea Level Change. In: *Climate Change 2013: The Physical Science Basis. Contribution of Working Group I to the Fifth Assessment Report of the Intergovernmental Panel on Climate Change* (Stocker, T.F., D. Qin, D., G.K. Plattner, G. K., M. Tignor, M., Allen, S. K., Boschung, J., Nauels, A., Xia, Y., Bex, V., and Midgley, P. M. (eds.)), Cambridge University Press, Cambridge, United Kingdom and New York, NY, USA, 2013.
- 20 Dansgaard, W.: Stable isotopes in precipitation, *Tellus*, XVI (4), 436-468, 1964.
- 25 Deb, P., A. Orr, J. S. Hosking, T. Phillips, J. Turner, D. Bannister, J. O. Pope, and S. Colwell, 2016: An assessment of the Polar Weather Research and Forecasting (WRF) Model representation of near-surface meteorological variables over West Antarctica. *J. Geophys. Res. Atmos.*, **121**, 1532–1548. Doi:10:1002/2015JD024037.
- Dittmann, A., E. Schlosser, V. Masson-Delmotte, J. G. Powers, K. W. Manning, M. Werner,
30 and K. Fujita. Precipitation regime and stable isotopes at Dome Fuji, East Antarctica. *Atmos. Chem. Phys.*, 16, 6883-6900, doi:10.5194/acp-16-688d3-2016, 2016.



- Enomoto, H., H. Motoyama, T. Shiraiwa, T. Saito, T. Kameda, T. Furukawa, S. Takahashi, Y. Kodama, and O. Watanabe. Winter warming over Dome Fuji, East Antarctica and semiannual oscillation in the atmospheric circulation. *J. Geophysic. Res.*, 103 (D18), 23,103-23,111, 1998.
- 5 EPICA community members: 8 Glacial cycles from an Antarctic ice core, *Nature*, 429, 623-628, 2004.
- Frieler, K., Clark, P. U., He, F., Buizert, C., Reese, R., Ligtenberg, S.R. M., Van den Broeke, M. R., Winkelmann, R., and Levermann, A.: Consistent evidence of increasing Antarctic accumulation with warming, *Nature Climate Change*, 5, 348-352,
10 doi:10.1038/NCLIMATE2574, 2015.
- Fudge, T. J., B. R. Markle, K. M. Cuffey, C. Buizert, K. C. Taylor, E. J. Steig, E. D. Waddington, H. Conway, and M. Koutnik: Variable relationship between accumulation and temperature in West Antarctica for the past 31,000 years. *Geophys. Res. Lett.*, 43, 3795-3803,
15 doi:10.1002/2016GL068356, 2016.
- Fujita, K., and Abe, O.: Stable isotopes in daily precipitation at Dome Fuji, East Antarctica, *Geophys. Res. Lett.*, 33, L18503, doi:10.1029/2006GL026936, 2006.
- 20 Gorodetskaya, I.V., N.P.M. Van Lipzig, M. R. Van den Broeke, A. Mangold, W. Boot, and C. H. Reijmer: Meteorological regimes and accumulation patterns at Utsteinen, Dronning Maud Land, East Antarctica: Analysis of two contrasting years. *J. Geophys. Res.*, 118, 1-16, doi:10.1002/jgrd.50177, 2013.
- 25 Hirasawa, N., Nakamura, H., and Yamanouchi, T.: Abrupt changes in meteorological conditions observed at an inland Antarctic station in association with wintertime blocking. *Geophys. Res. Lett.*, 27(13), 1911-1914, 2000.
- Hirasawa, N., Nakamura, H., Motoyama, H., Hayashi, M., and Yamanouchi, T.: The role of
30 synoptic-scale features and advection in a prolonged warming and generation of different forms of precipitation at dome Fuji station, Antarctica, following a prominent blocking event, *J. Geophys. Res.*, 118, 6916-6928, doi:10.1002/jgrd.50532, 2013.



- Jouzel, J. and L. Merlivat: Deuterium and oxygen 18 in precipitation: Modelling of the isotopic effects during snow formation. *J. Geophys. Res.*, 89, 11749-11757, 1984.
- Jouzel, J., R. B. Alley, K. M. Cuffey, W. Dansgaard, P. Grootes, G. Hoffmann, S. J. Johnsen,
5 R. D. Koster, D. Peel, A. Shuman, M. Stievenard, M. Stuiver, and J. White: Validity of the
temperature reconstruction from water isotopes in ice cores, *J. Geophys. Res.*, 102(C12),
26,471-26,487, 1997..
- Kuettel, M., E. Steig, Q. Ding, A. J. Monaghan, D. S. Battisti: Seasonal climate information
10 preserved in West Antarctic ice core water isotopes: relationships to temperature, large-scale
circulation, and sea ice. *Clim. Dyn.*, 39, 1841-1857, doi:10.1007/s00382-012-1460-7.
- Lorius, C., Merlivat, L., Jouzel, J., and Pourchet, M.: A 30,000 years isotope climatic record
from Antarctic ice, *Nature*, 280, (5724), 644-647, 1979.
15
- Massom, R., Pook, M. J., Comiso, J. C., Adams, N., Turner, J., Lachlan-Cope, T., and
Gibson, T.: Precipitation over the interior East Antarctic ice sheet related to midlatitude
blocking-high activity. *J. Climate*, 17, 1914-1928, 2004.
- 20 Merlivat, L. and J. Jouzel: Global climatic interpretation of the deuterium-oxygen 18
relationship for precipitation. *J. Geophys. Res.*, 84, 5029-5033, 1979
- Nicolas, J. P. and Bromwich, D. H.: Climate of West Antarctica and Influence of Marine Air
Intrusions. *J. Climate*, 24, 49-67. doi:10.1175/2010JCLI3522.1, 2011.
- 25 Nigro, M. A., Cassano, J. J., and Seefeldt, M. W.: A weather pattern-based approach to
evaluate the Antarctic Mesoscale Prediction System (AMPS) forecasts: Comparison to
automatic weather station observations. *Wea. Forecasting*, 26, 184-198,
DOI:10.1175/2010WAF2222444.1, 2011.
- Nigro, M. A., Cassano, J. J., and Knuth, S. L.: Evaluation of Antarctic Mesoscale Prediction
30 System (AMPS) cyclone forecasts using infrared satellite imagery. *Antarctic Science*, 24,
183-192, doi:10.1017/S0954102011000745, 2012.



- Noone, D., Turner, J., and Mulvaney, R.: Atmospheric signals and characteristics of accumulation in Dronning Maud Land, Antarctica. *J. Geophysic. Res.*, 104 (D16), 19,191-19,211, 1999.
- Powers, J. G., Monaghan, A. J, Cayette, A. M., Bromwich, D. H., Kuo, Y., and Manning, K. W.: Real-time mesoscale modeling over Antarctica. The Antarctic Mesoscale Prediction System. *Bull. Am. Meteorol. Soc.*, 84, 1522-1545, 2003.
- Powers, J. G.: Numerical prediction of an Antarctic severe wind event with the Weather Research and Forecasting (WRF) Model. *Mon. Wea. Rev.*, 135, 3134-3157, 2007.
- Powers, J. G., Manning, K. W., Bromwich, D. H., Cassano, J. J., and Cayette, A. M.: A decade of Antarctic science support through AMPS. *Bull. Amer. Meteor. Soc.*, 93, 1699-1712, 2012.
- Raphael, M., G. J. Marshall, J. Turner, R. L. Fogt, D. Schneider, D. A. Dixon, J. S. Hosking, J. M. Jones, and W. R. Hobbs: The Amundsen Sea Low. Variability, change, and Impact on Antarctic Climate. *Bull. Am. Meteorol. Soc.*, xx, 111-121, doi:10.1175/BAMS/D-14-00018.1, 2016.
- Reijmer, C. H. and van den Broeke, M. R.: Temporal and spatial variability of the surface mass balance in Dronning Maud Land, Antarctica. *J. Glaciol.*, 49(167), 512-520, 2003.
- Scarchilli, C., M. Frezzotti, and P. M. Ruti: Snow precipitation at for ice core sites in East Antarctica: Provenance, seasonality and blocking factors. *Clim. Dynam.* , 37, 2107-2125, doi:10.1007/s00382-010-0946-4, 2011.
- Schlosser, E., B. Stenni, M. Valt, A. Cagnati, J. G. Powers, K. W. Manning, M. Raphael, M. G. Duda. Precipitation and synoptic regime in two extreme years 2009 and 2010 at Dome C, Antarctica – implications for ice core interpretation. *Atmos. Chem. Phys.*, 16, 4757-4770, doi:10.5194/acpd-16-4757-2016, 2016.
- Schlosser, E., K. W. Manning, K. W., Powers, J. G., Duda, M. G., Birnbaum, G., and K. Fujita, . Characteristics of high-precipitation events in Dronning Maud Land, Antarctica. *J. Geophys. Res.*, 115, D14107, doi:10.1029/2009JD013410, 2010a.
- Schlosser, E., Powers, J. G., Duda, M. G., Manning, K. W., Reijmer, C.H., Van den Broeke, M.: An extreme precipitation event in Dronning Maud Land, Antarctica - a case study using



- AMPS (Antarctic Mesoscale Prediction System) archive data. Polar Research, doi:10.1111/j.1751-8369.2010.00164.x, 2010b.
- Schlosser, E., Duda, M. G., Powers, J. G., Manning, K. W.: The precipitation regime of Dronning Maud Land, Antarctica, derived from AMPS (Antarctic Mesoscale Prediction System) Archive Data. *J. Geophys. Res.*, 113. D24108, doi: 10.1029/2008JD009968, 2008.
- Seefeldt, M. W., and Cassano, J. J.: An analysis of low-level jets in the greater Ross Ice Shelf region based on numerical simulations. *Mon. Wea. Rev.*, **136**, 4188-4205. doi: 10.1175/2007JAMC1442.1, 2008.
- Seefeldt, M. W., and Cassano, J. J.: A description of the Ross Ice Shelf air stream (RAS) through the use of self-organizing maps (SOMs). *J. Geophys. Res.*, **117**, D09112. doi:10.1029/2011JD016857, 2012.
- Sime, L. C., G. J. Marshall, R. Mulvaney, and E. R. Thomas. Interpreting temperature information from ice cores along the Antarctic Peninsula: ERA40 analysis. *Geophys. Res. Lett.*, 36, L18801, doi:10.1029/2009GL038982, 2009.
- Steen-Larsen, H. C. , S. J. Johnson, S. J., Masson-Delmotte, V., Stenni, B., Risi, C., Sodemann, H., Balslev-Clausen, D., Blunier, T., Dahl-Jensen, D., Ellehøy, M. D., Falourd, S., Grindsted, A., Gkinis, V., Jouzel, J., Popp, T., Sheldon, S., Simonsen, S. B., Sjolte, J., Steffensen, J. P., Sperlich, P., Sveinbjörnsdottir, A. E., Vinther, B. M., White, J. W. C.: Continuous monitoring of summer surface water vapor isotopic composition above the Greenland Ice Sheet, *Atmos. Chem. Phys.*, 13, 4815-4828, 2013.
- Steen-Larsen, H. C., C. Risi, M. Werner, K. Yoshimura, and V. Masson-Delmotte: Evaluating the skills of isotope-enabled general circulation models against in situ atmospheric water vapor isotope observations. *J. Geophys. Res. Atmos.*, 122, doi:10.1002/2016JD025443, 2017.
- Stenni, B., Masson-Delmotte, V., Johnsen, S., Jouzel, J., Longinelli, A., Monnin, E., Roethlisberger, R., and Selmo, E.: An Oceanic Cold Reversal During the Last Deglaciation, *Science*, 293, 2074-2077, 2001.
- Stenni, B., Masson-Delmotte, V., Selmo, E., Oerter, H., Meyer, H., Roethlisberger, R., Jouzel, J., Cattani, O., Falourd, S., Fischer, H., Hoffmann, G., Iacumin, P., Johnsen, S. F., Minster,



B., and Udisti, R.: The deuterium excess records of EPICA Dome C and Dronning Maud Land ice cores (East Antarctica), *Quat. Scie. Rev.*, 29, 146-159, 2010.

Stenni, B., C. Scarchilli, V. Masson-Delmotte, E. Schlosser, V. Ciardini, G. Dreossi, P.
5 Grigioni, M. Bonazza, A. Cagnati, D. Karlicek, C. Risi, R. Udisti, and M. Valt: Three-year
monitoring of stable isotopes of precipitation at Concordia Station, East Antarctica. *The
Cryosphere Discuss.*, doi:10.5194/tc-2016-142, 2016.

Stoelinga, M. T.: A users guide to RIP Version 4.5: A program for visualizing mesoscale
model output. NCAR online document. University of Washington.

10 http://www.mmm.ucar.edu/mm5/documents/ripug_V4.html, 2009.

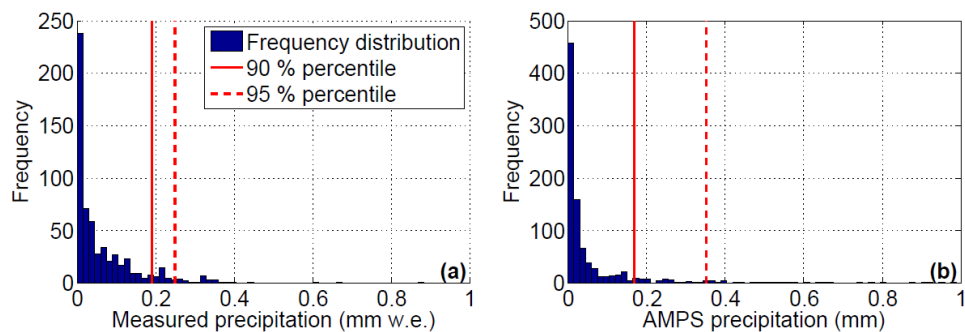
Wendler, G. and Y. Kodama: On the climate of Dome C, Antarctica, in relation to its
geographical setting. *Intern. J. Climat.*, 4, 495-508, doi:10.1002/joc.3370040505, 1984.

15

20

25

30



5

Figure 1: Histogram of daily precipitation amounts for a) measurements and b) AMPS archive data corresponding to the period 2008-2010.

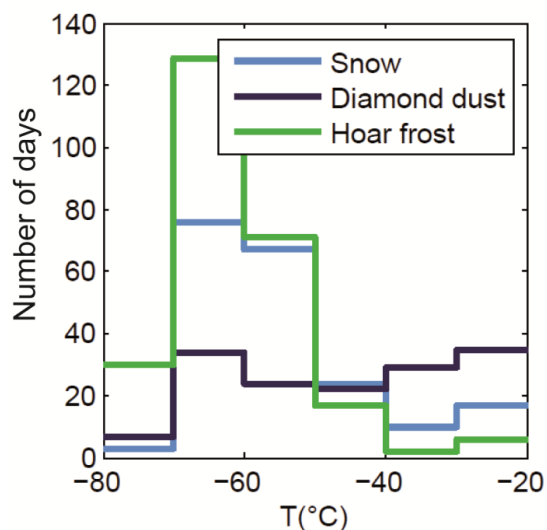


Figure 2: Frequency of the different precipitation types

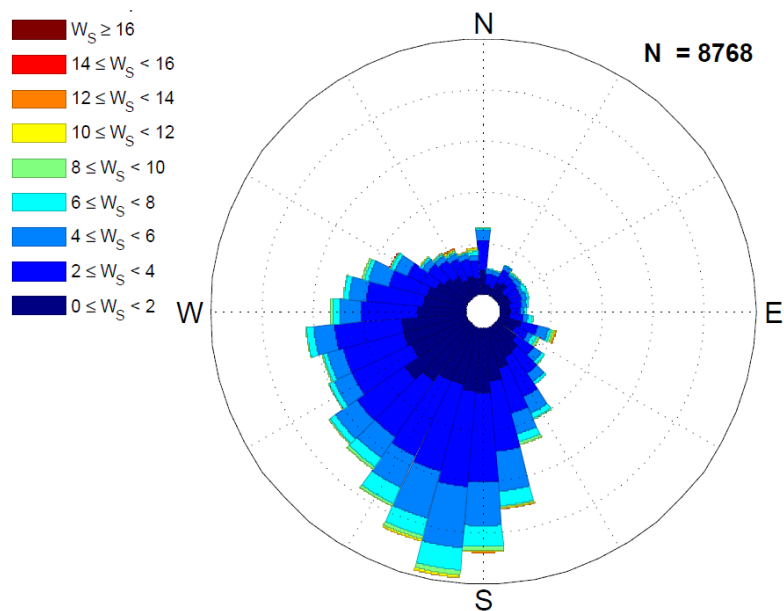
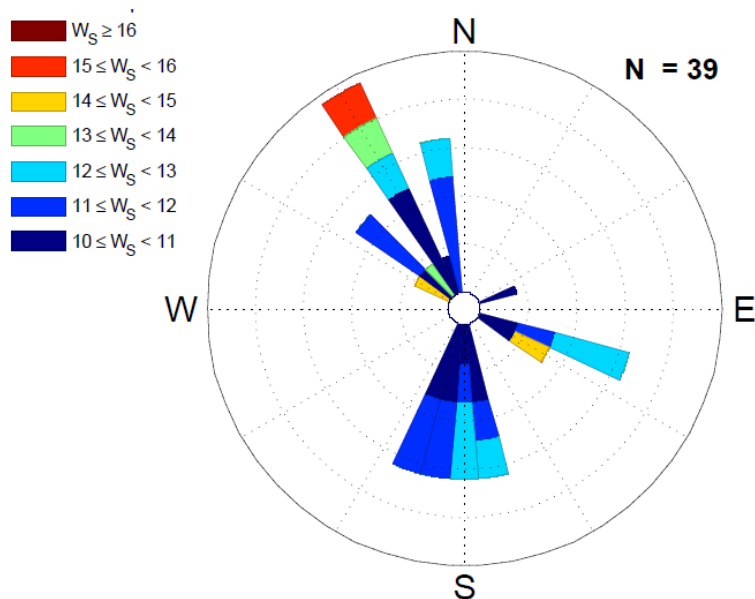


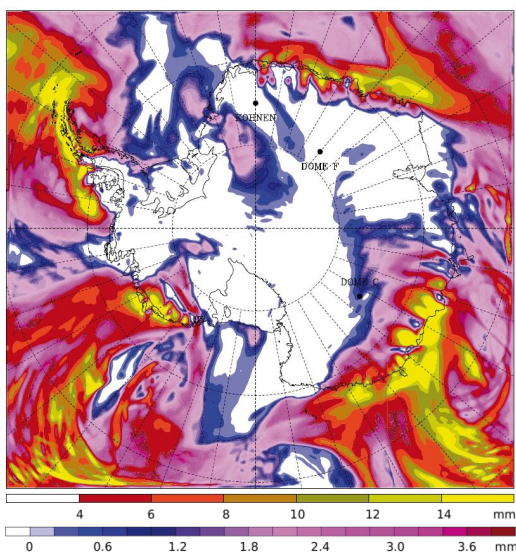
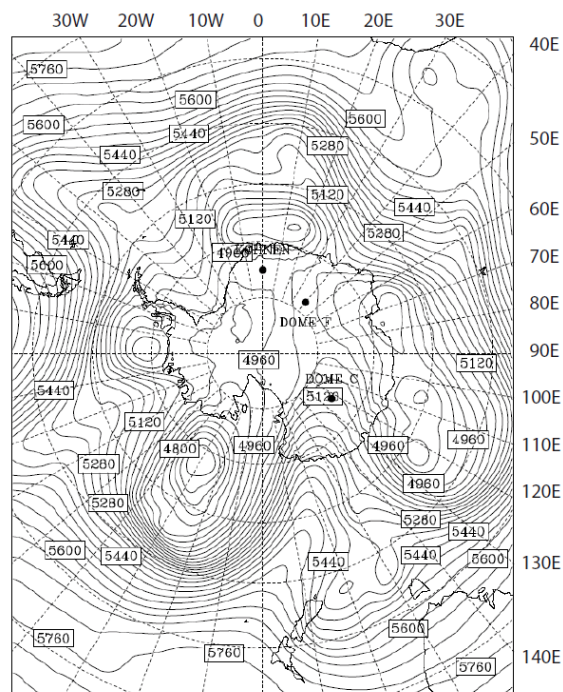
Figure 3a): Observed wind speed W_s and direction at Dome C AWS



5 Figure 3b): Observed wind speed W_s and direction for cases with wind speeds larger than 10 m s^{-1}

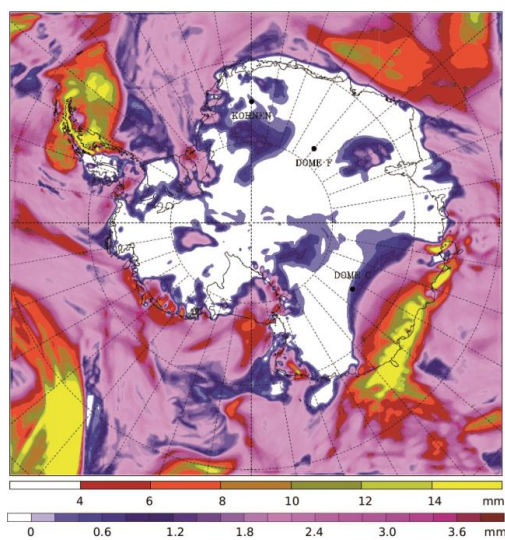
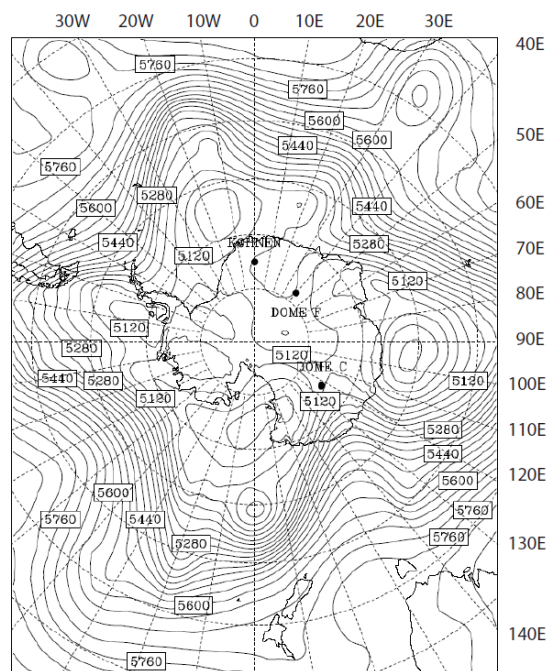


a) blocking high 23 May 2007 00Z



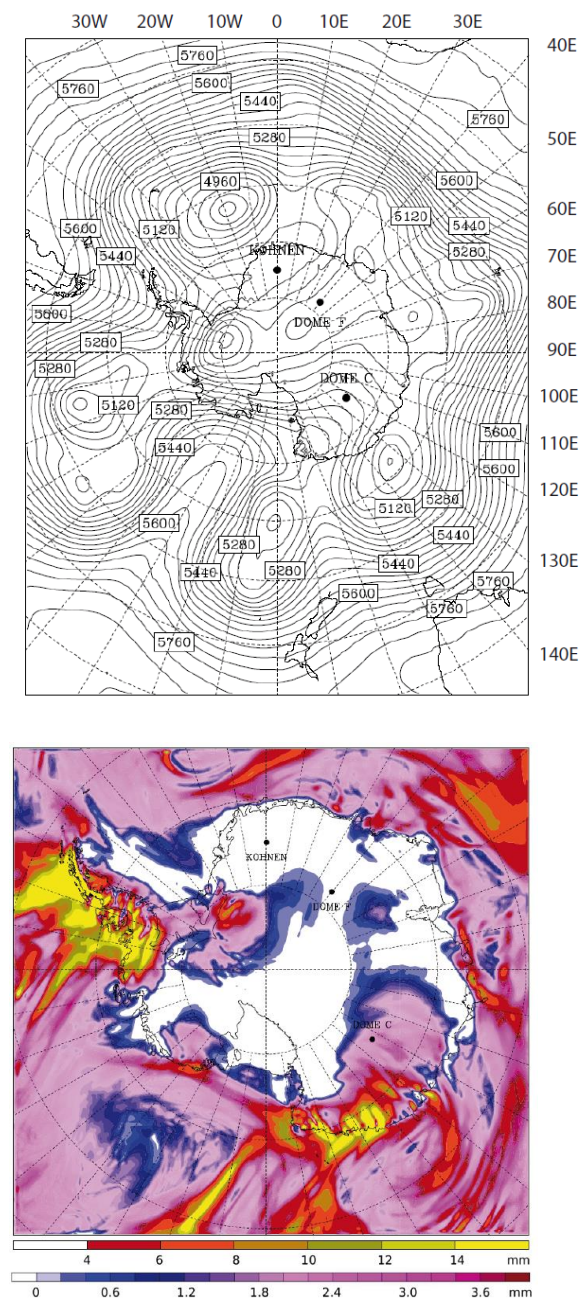


b) weak anticyclone with northwesterly flow



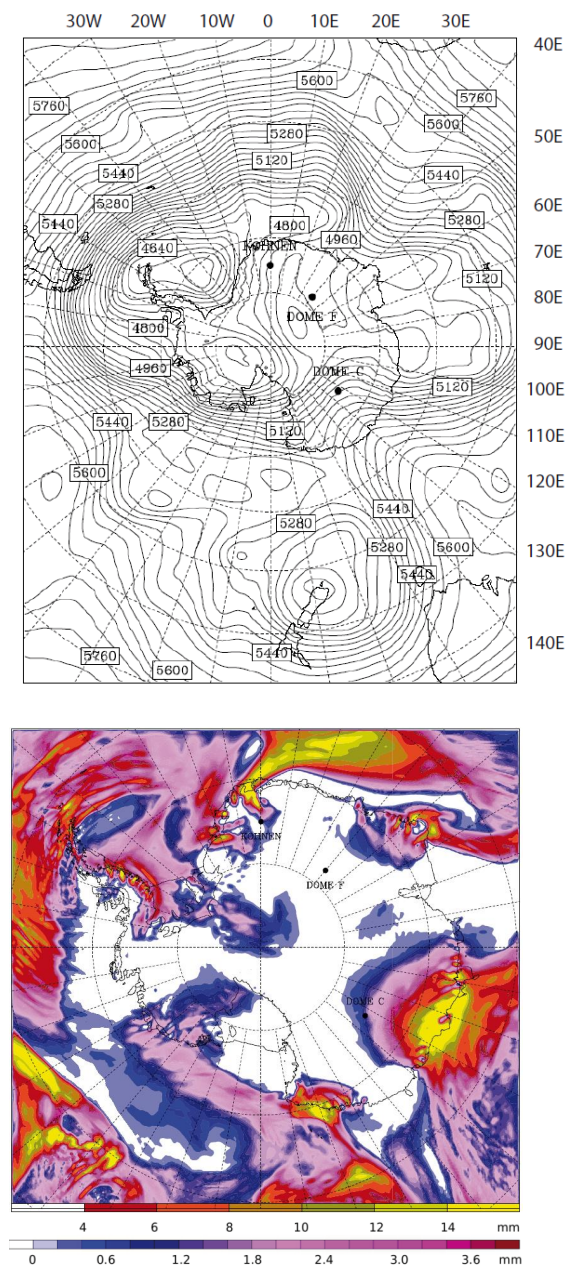


c) anticyclone with northeasterly flow 15 Mar 2007 00Z



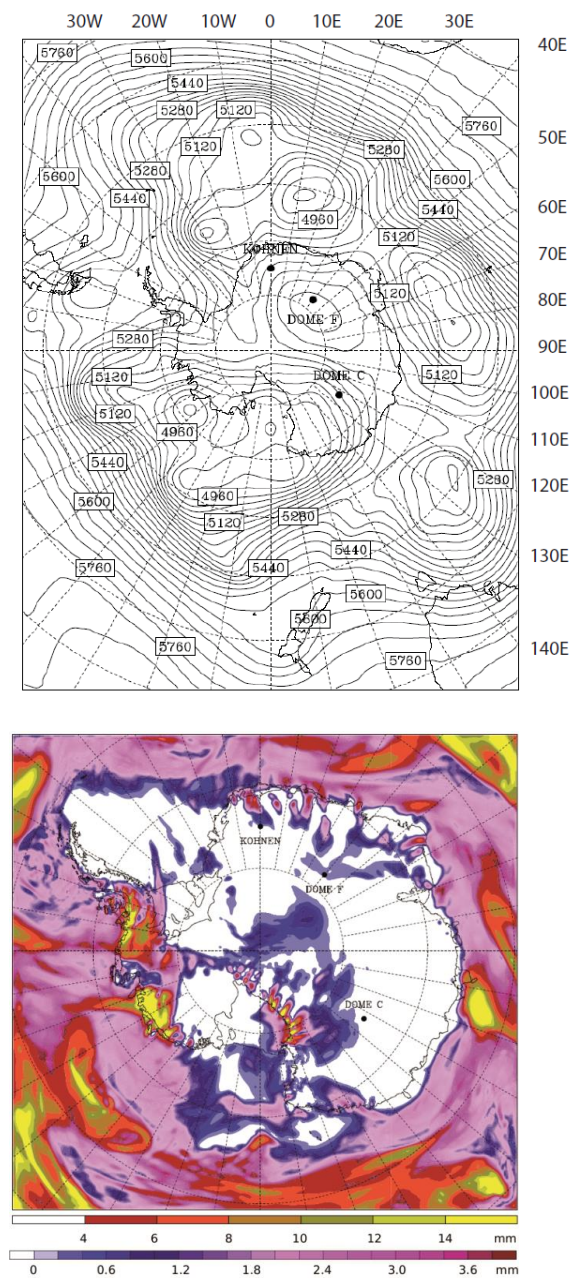


d) splitting of flow





e) southerly flow from West Antarctica





f) post event

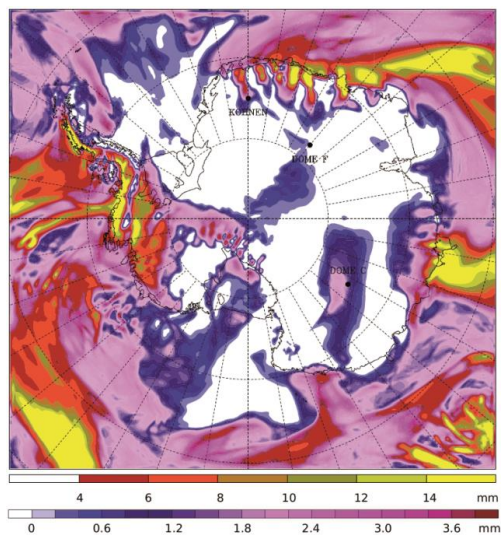
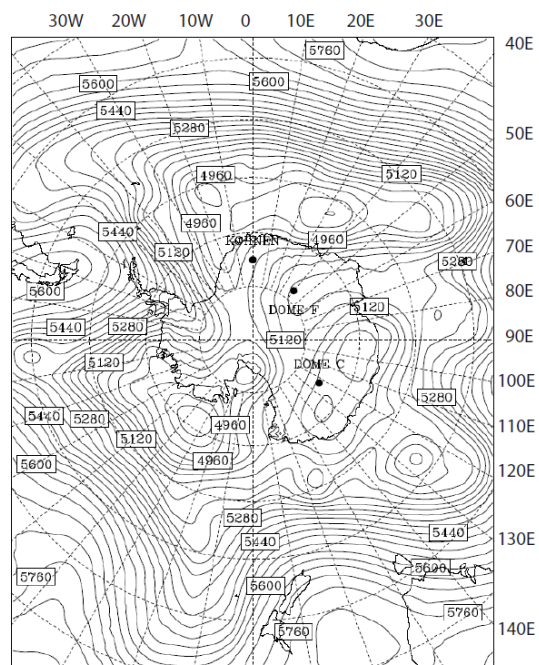




Figure 4: Synoptic patterns classification

500 hPa geopotential height (contour interval 10gpm) and 24h precipitation totals from AMPS archive for the different synoptic situations during precipitation:

- a) blocking anticyclone with northwesterly flow (23 May 2007)
 - 5 b) weak anticyclone with northwesterly flow (13 Feb 2007)
 - c) anticyclone with northeasterly flow (16 Mar 2007)
 - d) splitting of flow (14 Aug 2008)
 - e) southerly flow from West Antarctica (3 May 2007)
 - f) post event (28 May 2007)
- 10 500 hPa geopotential height fields stem from AMPS 12h forecast of the preceding day, corresponding to 00 UTC of the described day, precipitation is AMPS 12h-36h forecast of the preceding day, corresponding to 00-24 UTC of the day described.

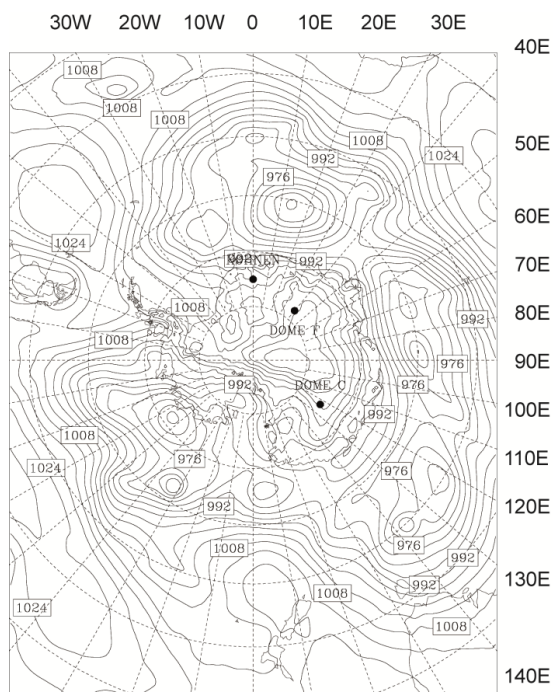


Figure 5: Sea level pressure from AMPS (domain 1) for 3 May 2007 00 UTC

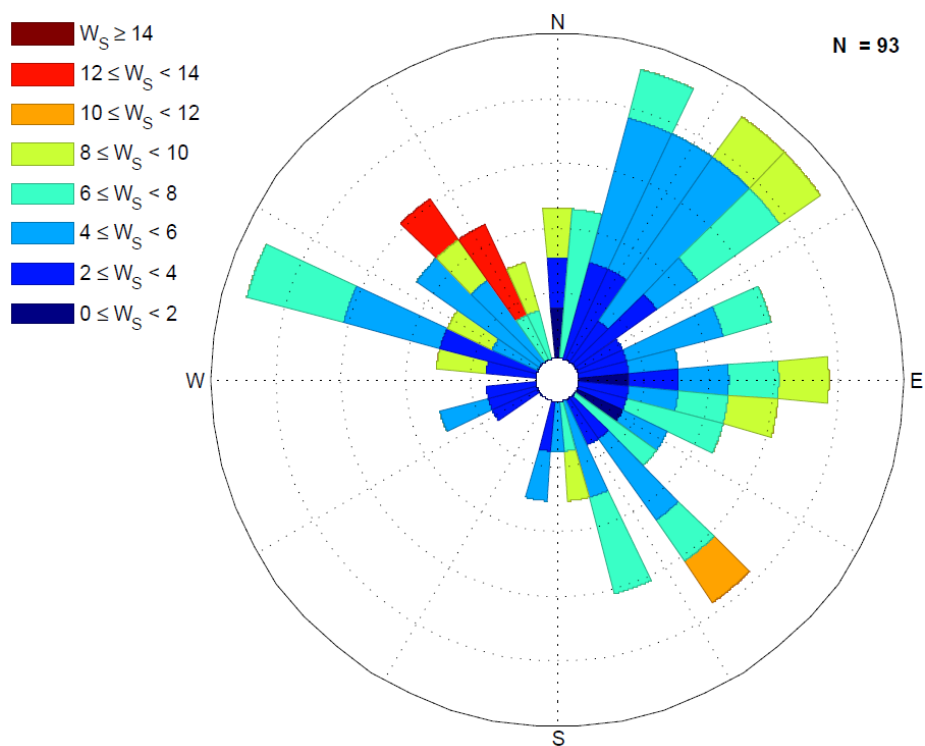


Figure 6: Wind speed W_s and direction for snowfall events identified in AMPS data

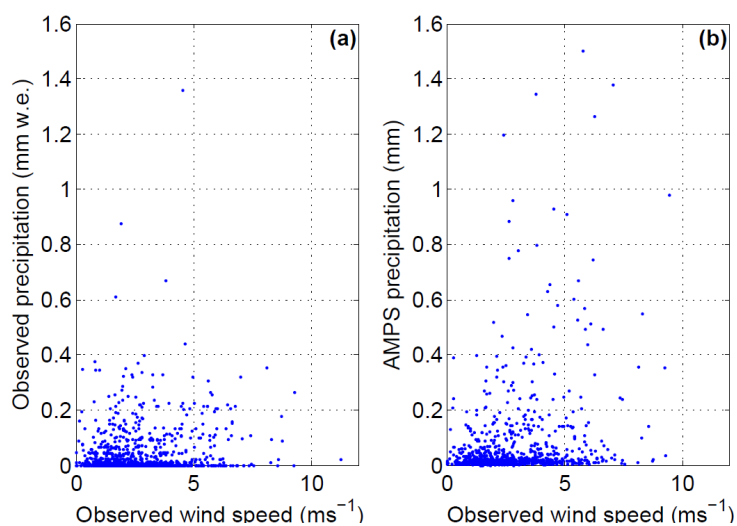


Figure 7: Observed wind speed at AWS vs. observed and modelled 24h – precipitation at

5 Dome C

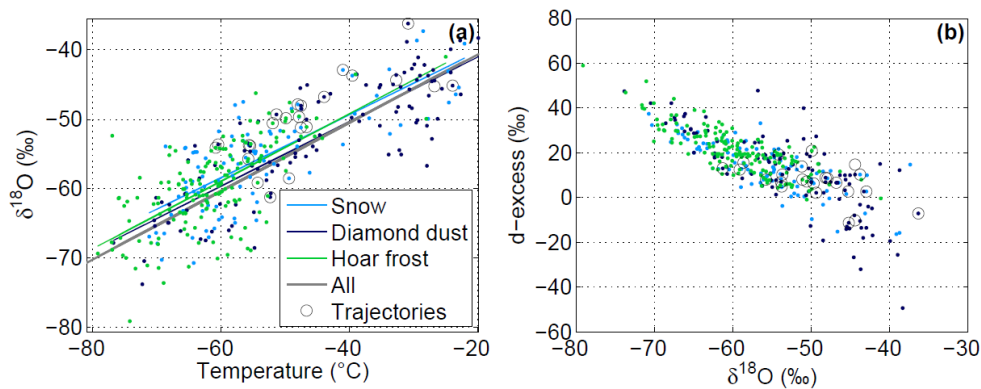
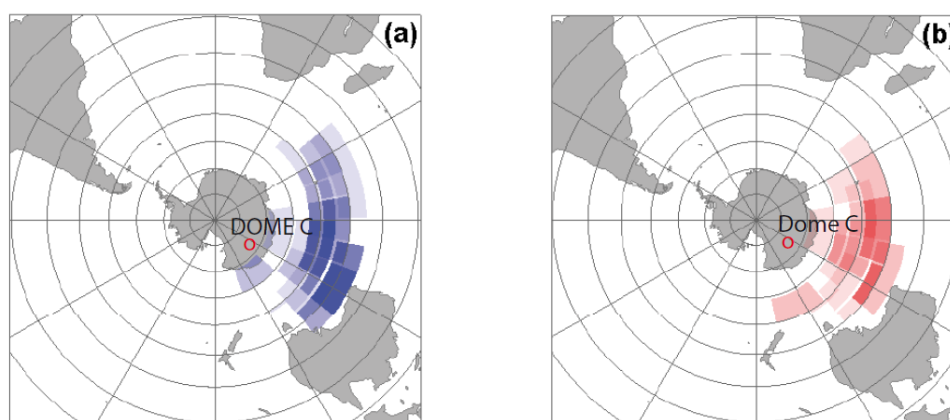


Figure 8:

- a) $\delta^{18}\text{O}$ of precipitation samples vs. 2m air temperature from AWS for the different types of precipitation, snow, diamond dust, and hoar frost. Cases, for which trajectories were calculated, are marked with circles.
- b) $\delta^{18}\text{O}$ of precipitation samples vs. deuterium excess

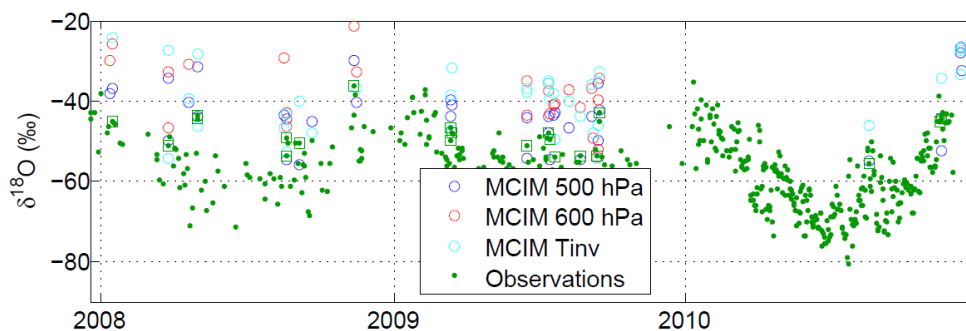


10

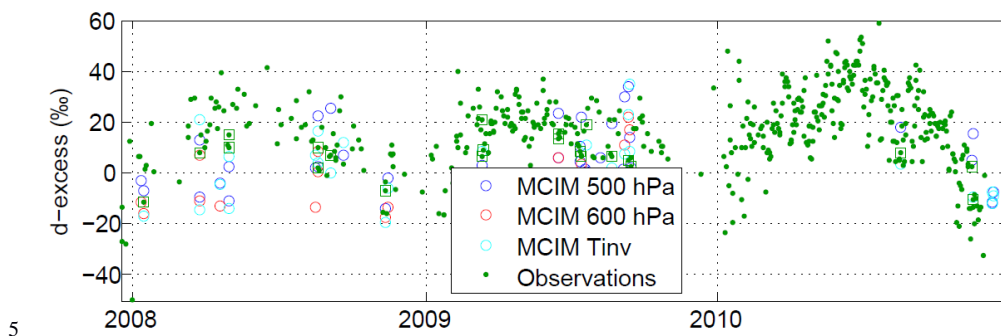
Figure 9: Estimated moisture source areas for arrival levels a) 600 hPa and b) 500 hPa. Stronger colour corresponds to higher frequency of occurrence of the respective moisture source.



a)



b)



5
10 **Figure 10: Observed and modelled a) $\delta^{18}\text{O}$ and b) deuterium excess for days with moisture source estimates with Dome C temperature taken at 500hPa level, 600hPa level, and at the upper limit of the temperature inversion layer (derived from radiosondes as described in the text). The green squares mark days, for which trajectory calculations were carried out.**